Carbohydrate Polymers 102 (2014) 746–754

Contents lists available at ScienceDirect

Carbohydrate Polymers

journal homepage: www.elsevier.com/locate/carbpol

Thermal properties and crystallization behavior of thermoplastic starch/poly(ε-caprolactone) composites

Jie Cai[a,b,c,**], Zhouyi Xiong[a], Man Zhou[a,b], Jun Tan[a], Fanbing Zeng[d], MeihuMa[a], Shun Lin[a,b], Hanguo Xiong[a,b,*]

[a] College of Food Science and Technology, Huazhong Agricultural University, Wuhan 430070, China
[b] Research Institute of Comprehensive Utilization of Biomaterials, Huazhong Agricultural University, Wuhan 430070, China
[c] Institute for Frontier Materials, Deakin University, Geelong, VIC 3220, Australia
[d] College of Science, Huazhong Agricultural University, Wuhan 430070, China

ARTICLE INFO

Article history:
Received 1 August 2013
Received in revised form 20 October 2013
Accepted 30 October 2013
Available online 7 November 2013

Keywords:
Thermoplastic starch
Poly(ε-caprolactone)
Thermal properties
Crystallization behavior

ABSTRACT

TPS/PCL composites were prepared by PCL melt blending with modified corn starch. The structure, thermal properties, morphology and crystallization behavior of these composites were investigated by FTIR, TGA, SEM, XRD and DSC. FTIR confirmed the existence of the interaction between PCL and TPS, whereas TGA showed that the thermal stability was decreased by the addition of TPS. Meanwhile, SEM showed a weak interfacial adhesion with increasing TPS. According to the Avrami theory, TPS functioned as a nucleating agent to improve the crystallinity rate of PCL. However, the XRD analysis revealed that the crystallinity decreased. At the same time, the ΔE_a of the composites was higher than those of neat PCL. These changes in values all indicated that mobility constraints existed in the PCL chains with the increasing of TPS, which leaded to a drop in the crystallization ability of PCL.

1. Introduction

With the increasing development of technology in petrochemical polymers, the consumption of non-renewable materials in various applications has generated considerable environmental problems (Ke & Sun, 2000; Kumar, Mohanty, Nayak, & Parvaiz, 2010; Suprakas, Kazunobu, Masami, Akinobu, & Kazue, 2003; Zou, Tang, Fu, & Xiong, 2009). Recently, considerable researches have been devoted to finding innovative ways to efficiently use natural polymers in industrial and technical areas. Moreover, these studies involve theoretical investigations whose primary aim is to address these problems in the polymer industry (Tamai, Aono, Tatsumi, & Matsumoto, 2003).

Poly(ε-caprolactone) (PCL) is one of the most promising candidates currently available in the market for environment-friendly composite development, especially in the packaging sector (Del et al., 2009; Flemming, 1998; Joseph et al., 2011; Rhim, Park, & Ha, 2013). In this sector, the use of PCL is highly encouraged by environmental management policies. Unlike petroleum-based plastics, PCL is a synthetic, biodegradable polyester that is compatible with many types of polymers. However, relatively high costs and low melting temperature (around 60 °C) are major defect limitations of PCL, which prevent its widespread industrial use and lower the possibility of commercialization. Studies on PCL mixed with other low-cost biodegradable material have been usually carried out to broaden PCL applications (De, Vander, & David, 1997; Mahieu, Terrié, Agoulon, Leblanc, & Youssef, 2013; Nakayama et al., 1997).

As an abundant low-cost polymeric material, natural starch has numerous distinguishing features. Natural starch has been widely used as the filler in polymers, such as the composites of starch/PE (Peter, Krishnan, & Debes, 2009; Wang & Yu, 2005), starch/LDPE (Heartwin, Pratik, & Milford, 2010; Huang, Roan, Kuo, & Lu, 2005; Nakamura, Cordi, Almeida, Duran, & Mei, 2005; Pedroso & Rosa, 2005) and starch/PVA (Cao, Mohamed, Gordon, Willett, & Sessa, 2003; Elsenhaber & Schulz, 1993; Leloup, Colonna, & Ring, 1991; Liu et al., 2012; Luo, Li, & Lin, 2012; Xiong, Tang, Tang, & Zou, 2008; Yoon, Park, & Byun, 2012). Starch exists in granular form, thus the molecular order within the granules must be destroyed to improve its processability. Hence, a common/most frequently used approach of modification starch is heating with plasticizers.

Thermoplastic starch/poly(ε-caprolactone) (TPS/PCL) composite materials prepared by PCL melt blending with modified corn starch (CS) are expected to improve their respective undesirable

* Corresponding author at: College of Food Science and Technology, Huazhong Agricultural University, Wuhan 430070, China. Tel.: +86 27 87288377; fax: +86 27 87286608.
** Corresponding author at: College of Food Science and Technology, Huazhong Agricultural University, Wuhan 430070, China. Tel.: +86 13297099332; fax: +86 27 82353128.
E-mail addresses: xionghanguo@163.com (H. Xiong), caijievip@hotmail.com (J. Cai).

0144-8617/$ – see front matter © 2013 Elsevier Ltd. All rights reserved.
http://dx.doi.org/10.1016/j.carbpol.2013.10.095

properties and exhibit a particular synergistic effect. This composite has the potential to economize petroleum resources, and to develop new nonfood uses for starch. In this study, the effects of thermoplastic starch (TPS) on the structure, thermal properties, morphology and crystallization behavior of TPS/PCL composites were investigated by Fourier transform infrared (FTIR) spectroscopy, thermogravimetric analysis (TGA), scanning electron microscopy (SEM), X-ray diffraction (XRD) and differential scanning calorimetry (DSC).

2. Experimental methods

2.1. Materials

Poly(ε-caprolactone) (PCL) ($M_n = 7 \times 10^4$) pellets used in this investigation were acquired from Daicel Chemical Industries and had been dried in an air oven at 50 °C for 24 h. Meanwhile, granular (native) corn starch (CS) was supplied by Research Institute of comprehensive utilization of Biomaterials, Huazhong Agricultural University, China. CS was modified to obtain thermoplastic starch (TPS) by using glycerol (glycerol/CS 3/100 by weigh).

2.2. Preparation of TPS/PCL composites

The TPS and PCL were then mixed by the Stirring Kneader (NH-20 Rugao Tong-da Machinery Manufacturing, China) at 80 °C for 10–15 min. The ratios of TPS/PCL were 0/10, 2/10, 4/10 and 6/10, as SP0, SP2, SP4 and SP6, respectively. The resulting sheet was compressing molded at 80 °C into 1–1.5 mm thick sheet under a pressure of 20 MPa for 5 min, and then kept at room temperature.

2.3. Fourier transform infrared (FTIR) spectroscopy

FTIR spectra were recorded, at room temperature, in a Nicolet (USA) Nexus 470 FTIR spectrometer, with resolution of 4 cm^{-1} and averaged over 32 scans in the range 4000–400 cm^{-1}. The powdered samples were thoroughly grounded with potassium bromide (KBr) and laminated.

2.4. Thermogravimetric analysis (TGA)

TGA scans were obtained using 5–7 mg of each sample run from 25 °C to 600 °C at a heating rate of 10 °C/min under a nitrogen atmosphere in a TA 2900 instrument. The temperatures at which mass loss occurred (T_α) were determined directly from the thermograms.

2.5. Scanning electron microscopy (SEM)

The microstructure of fracture surfaces of TPS/PCL composites were examined using a JSM-6390LV (Japan) instrument operating at an acceleration voltage of 20 kV. The samples were cooled in liquid nitrogen, and then broken. The fracture surfaces were sputter coated with gold prior to SEM analysis.

2.6. X-ray diffraction measurement (XRD)

X-ray diffraction (XRD) patterns were recorded with a Rigaku (Japan) D/max-RB X-ray diffractometer in the angular range 5–60° (2θ) at ambient temperature, and Cu Kα tangent was used at 40 KV and 40 mA. The measurement was performed at a scanning speed of $2\theta = 10^\circ$ min^{-1}.

2.7. Differential scanning calorimetry analysis (DSC)

The thermal properties of the samples were conducted using a Nexus DSC 204F1 in nitrogen gas atmosphere. Samples of 5–10 mg were encapsulated into aluminum pans and were heated from 25 °C at the rate of 10 °C/min to 95 °C above the melting temperature (around 60 °C) and then kept at this temperature for 5 min to eliminate previous thermal history of melt characterization. And then samples were rapidly cooled down to the designated crystallization temperature (T_c) of interest 40, 41 and 42 °C at the rate of 10 °C/min to obtain the crystallization curve, respectively. The sample was held at desired isothermal temperature for the completion of the crystallization process until the crystallization process was no changed in the heat flow. All the thermograms are presented with downward deflection in DSC scans.

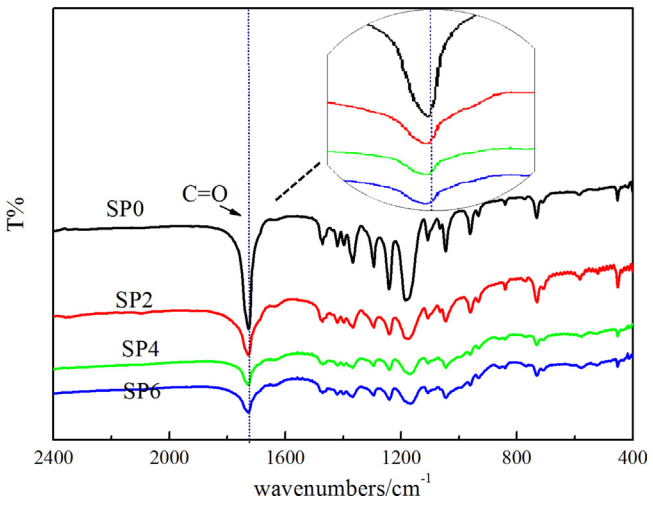

Fig. 1. FTIR spectrum of SP0, SP2, SP4 and SP6.

3. Results and discussion

3.1. FTIR spectroscopy analysis

FTIR spectroscopy was used to investigate the interaction of polymer blends, which could indicate segment interactions and provide information about the phase behavior of polymer blends.

Fig. 1 shows the FTIR spectrum of SP0, SP2, SP4 and SP6 in specific stretching regions. The spectrum of SP2, SP4 and SP6 are all similar to SP0. It is well known that PCL has a strong carbonyl stretching absorption at about 1726 cm^{-1}. With the addition of TPS, this peak shifted to a higher wavenumber (zoom in). This means that carbonyl groups take part in the interaction between PCL and TPS, resulting in the blue shift of the —C=O vibration of PCL.

3.2. TGA study

TGA has proved to be a suitable method to investigate the thermal stability of polymeric systems (Mano, Koniarova, & Reis, 2003).

The thermogravimetric (TG)/derivative thermograms (DTG) curves of pure PCL and PCL blends are shown in Fig. 2(a) and (b) at a heating rate of 10 °C/min in an N_2 atmosphere, respectively. The amount of weight loss in TG process is equal to the integral of the DTG curve against temperature. The area under each peak represents the weight loss of each component. From the DTG curves, PCL exhibits only one degradation peak, whereas PCL blends has three peaks, corresponding to the three steps in TG curve. The first peak at 281 °C is attributed to the maximum degradation rate (T_{max}), due to the loss of low weight compounds such as additives. The second and third peaks were attributed to starch (T_{max} = 321 °C), and PCL (T_{max} = 414 °C), respectively, by comparing with the values of the pure PCL determined in the same conditions.

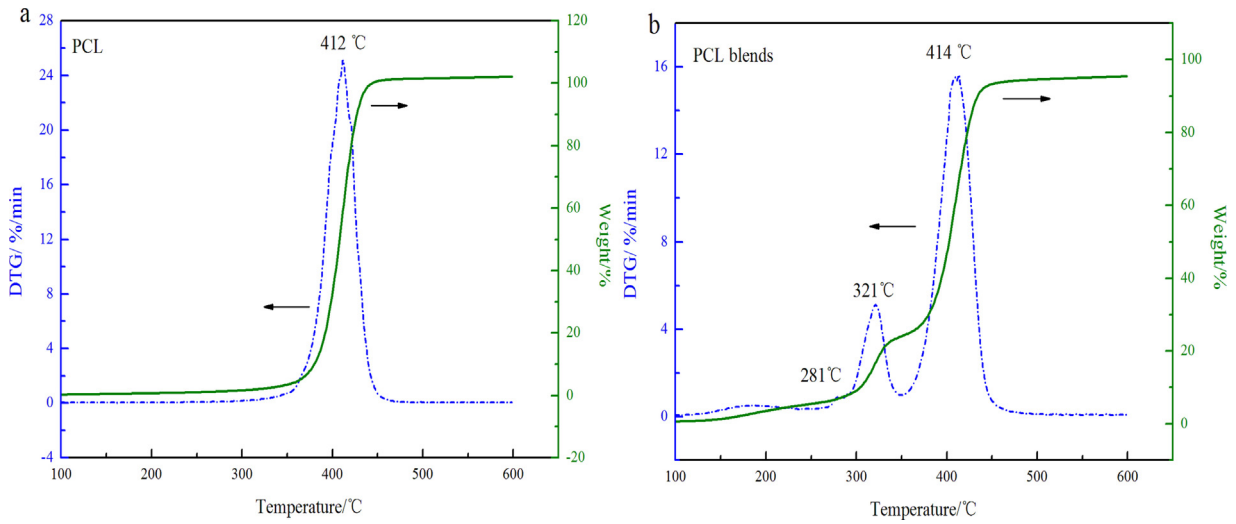

Fig. 2. TG/DTG curves obtained at 10 °C/min under nitrogen atmosphere: (a) pure PCL; (b) PCL blends.

Fig. 3 is the traces obtained in the TGA analysis which show the mass loss versus temperature for SP0, SP2, SP4 and SP6 with different TPS content. The change in onset of the thermal degradation of PCL (from 376 to 278 °C) when mixed with TPS was quite remarkable. This was expected since the components from natural sources burn at lower temperature than the synthetic ones, like PCL. In addition, it is possible to observe that the PCL/TPS blends present the same degradation profile, with the initial mass loss close to 100 °C, probably due to the presence of water that is linked by hydrogen bonds to the hydrophilic components, such as starch and part of the protein chain. Like many polyesters, this type of interaction is very poor, since they are hydrophobic. It can be seen that the thermal degradation of SP4 and SP6 starts close to 278 °C and develops in two stages, different from pure PCL, probably because of the addition of other components to PCL that interfere with the degradation mechanism.

In Fig. 3a, the losses in mass for the SP0, SP2, SP4 and SP6 blends at 376 °C were 8.12, 13.26, 23.52 and 28.50%, respectively, indicating that an increase in TPS content increased the loss of the blend. In other words, the pure PCL exhibited a higher thermal stability than the blend composites. The thermal stability follows the sequence SP0 > SP2 > SP4 > SP6. It concluded that the addition of TPS is responsible for the reduction in thermal stability of the blend since the temperature of thermal degradation of starch is about 260 °C (Avella, Errico, Rimedio, & Sadocco, 2002)

Fig. 4a shows the temperatures at 10, 20, 30, 40 and 50% losses in mass for PCL and their composites. It was also found that an increase in TPS content increased the loss of mass in the composite and decreased the thermal stability of PCL blends.

The activation energy of decomposition, E_t, of the polymer could be calculated from the TGA curves by the integral method proposed by Horowitz and Metzger (Horowitz & Metzger, 1963) using the following equation:

$$\ln[\ln(1-x)^{-1}] = \frac{E_t(T - T_{max})}{RT_{max}^2} \quad (1)$$

where x is the decomposed fraction, T is the temperature and R is the gas constant. From the plots of $\ln[\ln(1-x)^{-1}]$ versus θ ($\theta = T - T_{max}$), which are shown in Fig. 4b, E_t could be determined (from the slopes of the straight lines). As demonstrated in Table 1, the E_t values of PCL decreased dramatically after processing. This suggests that the addition TPS could decrease the thermal stability of PCL blends.

The weight percentage of char residues for all samples is presented in Fig. 3b to verify that the presence of TPS affects thermal stability. It was observed that the percent ash content increased from 0.06% to 4.68% (SP2 to SP6), with an increase in TPS content. It may be due to the fact that the starch is a carbohydrate, which yields high charred products.

3.3. Morphology of the composites

The SEM micrographs of the cryo-fractured surfaces (Fig. 5) show that the addition of TPS in different concentrations (Fig. 5b and c), decreases the homogeneous phase of pristine PCL (Fig. 5a);

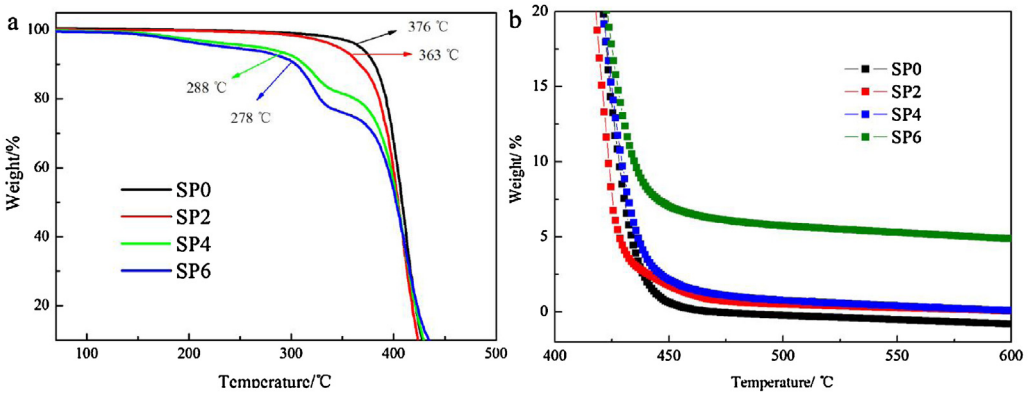

Fig. 3. TGA curves for SP0, SP2, SP4 and SP6.

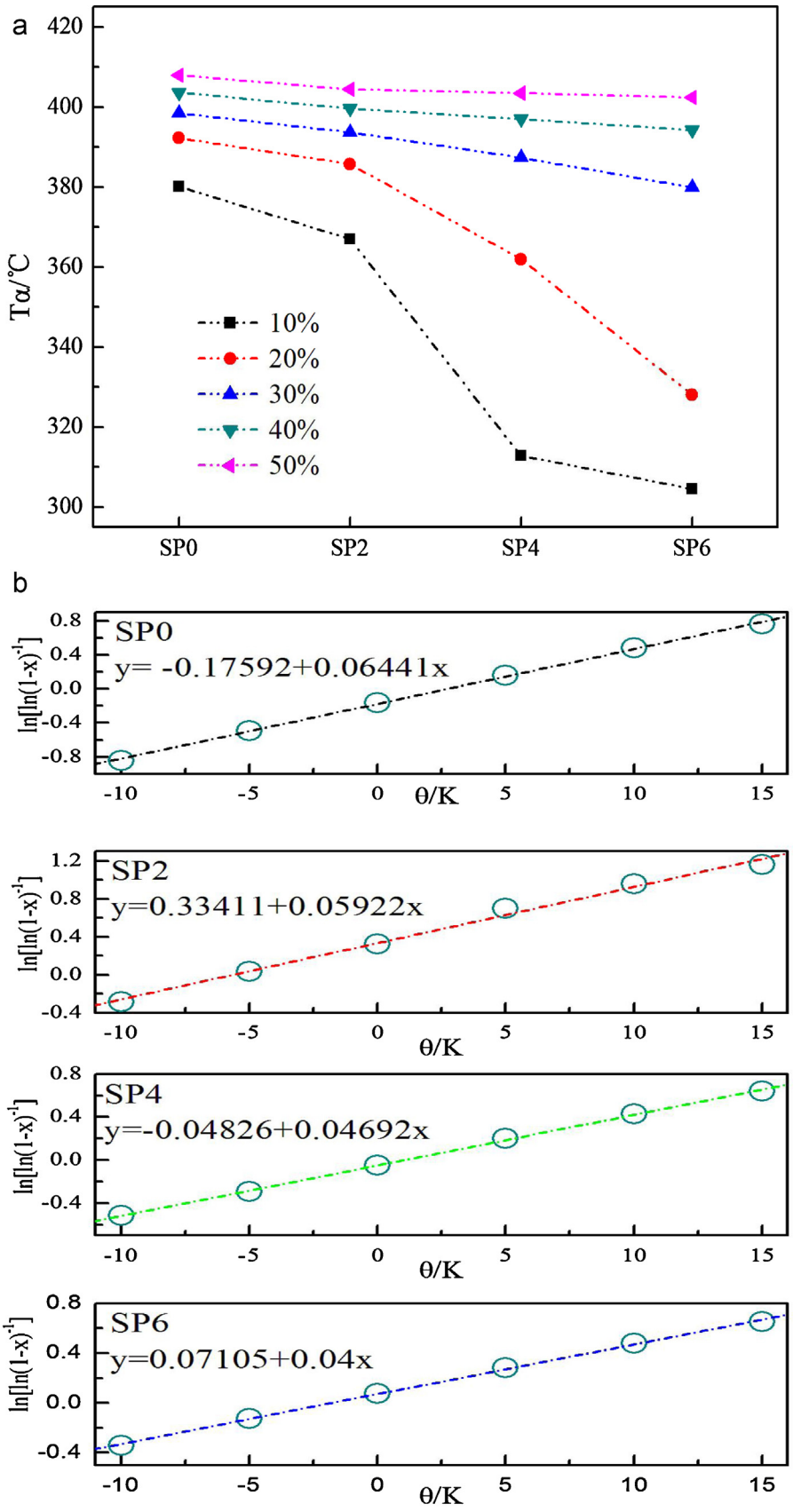

Fig. 4. (a) Influence of temperature on the loss of mass by SP0, SP2, SP4 and SP6. (b) Plots of $\ln[\ln(1-x)^{-1}]$ versus θ for the determination of E_t. The straight line is the linear fit of the data points.

Table 1
Thermogravimetry and dynamic isothermal crystallization parameters for SP0, SP2, SP4 and SP6.

Samples	E_t (kJ/mol)	T_c (°C)	$t_{1/2}$ (min)	G (min^{-1})	n	K (min^{-1})	ΔE (kJ/mol)
SP0	250.74	40	2.27	0.32	2.31	0.10	−231.19
		41	3.11	0.32	1.83	0.09	
		42	3.82	0.26	1.81	0.06	
SP2	233.58	40	1.16	0.86	2.4	0.48	−486.12
		41	2.11	0.47	2.5	0.11	
		42	3.71	0.27	2.1	0.05	
SP4	182.06	40	0.84	1.19	2.3	1.03	−470.84
		41	1.28	0.78	2.6	0.37	
		42	2.70	0.37	2.6	0.06	
SP6	156.58	40	0.64	1.57	2.2	1.83	−412.88
		41	1.52	0.66	2.5	0.25	
		42	1.78	0.56	2.4	0.17	

but it also shows a homogeneous dispersion of TPS in the matrix. All of the blends had good dispersion of the polymers (SP2 and SP4), although two distinct phases containing PCL and starch were seen (Fig. 5c).

Fig. 5b shows good interfacial adhesion between PCL and TPS melt phases. This could be due to the hydrogen bonding interactions between the ester carbonyl of PCL and the —OH groups on starch. This interaction leads to lowering the interfacial tension between PCL and TPS melt phases, leading to compatibilization. This compatibilization explains the blue shift of the —C=O vibration of PCL as shown in FTIR analysis.

With increasing TPS content, the differences in the phases were accentuated (Fig. 5c), although the molecular interactions still exist in the system. Fig. 5c shows cavities on the fractured surface of

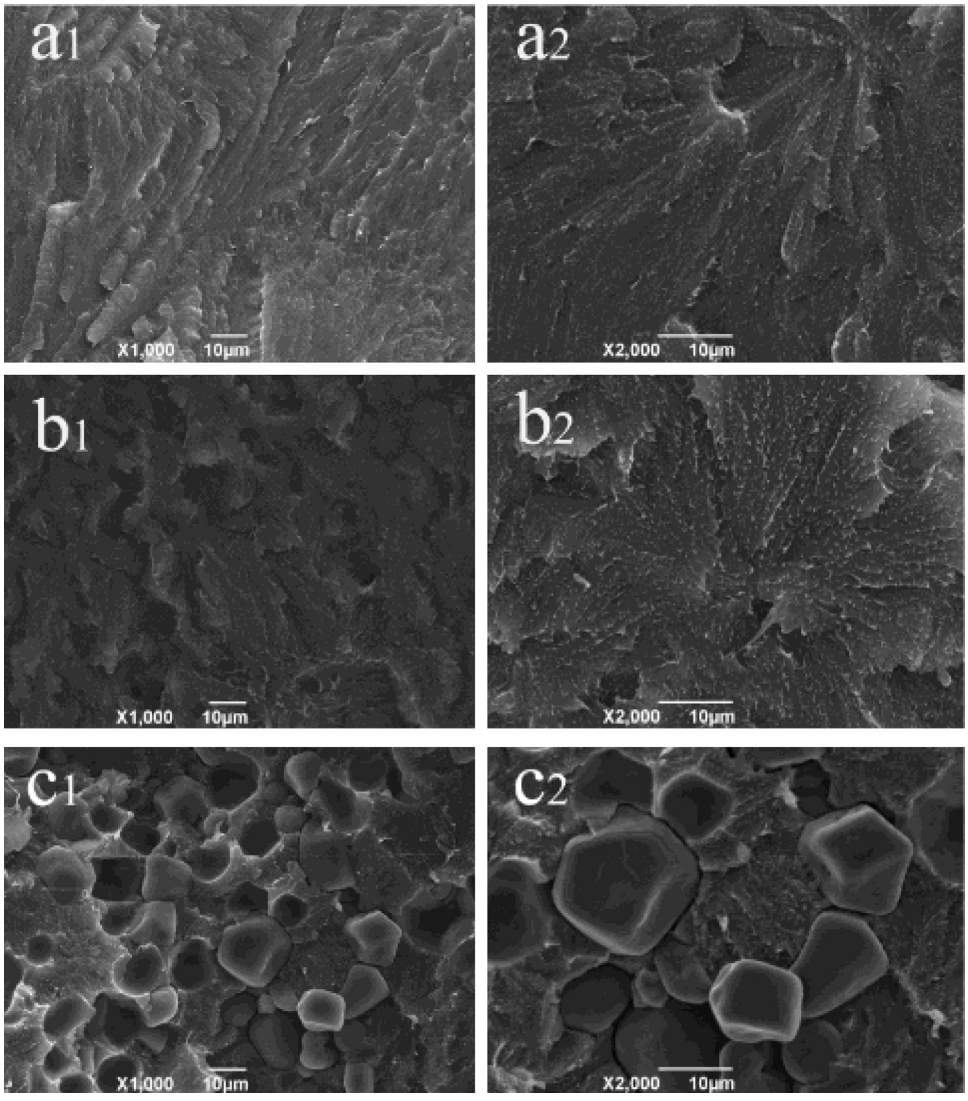

Fig. 5. SEM micrographs of the fractured surface of: SP0 (a), SP2(b) and SP4 (c).

the blend. These cavities were caused by the spontaneous detachment of TPS from PCL, and indicated weak interfacial adhesion between PCL and TPS. Some corresponding research also demonstrated that the interfacial bonding in PCL/starch blends was poor (Ishiaku, Pang, Lee, & Ishak, 2002; Rosa, Rodrigues, & Guedes, 2003). In this case, large spaces surrounded the starch granules gave the impression that the latter were situated in oversized cavities. Many granules had also been removed from these cavities. In addition to this, the poor interfacial bonding could have an influence on inferior the thermal stability of the blends, compared to the pure polymers.

3.4. XRD analysis

X-ray diffraction (XRD) patterns of PCL and TPS/PCL composites are shown in Fig. 6a. The crystallinity degree (X_c') of the composites was calculated by the crystalline and non-crystalline areas:

$$X_c' \ (\%) = \frac{I_c}{I_c + I_a} \times 100 \tag{2}$$

where I_c is the area of crystalline, I_a is the area of non-crystalline.

As shown in Fig. 6a, the patterns of pure PCL displayed sharp and strong crystalline peaks at about 21.70 and 24.07, which are ascribed to the {1 1 0} and {2 0 0} crystallographic planes, respectively. Thus, pure PCL has a higher crystallinity degree. The patterns of TPS/PCL composites showed similar peaks at 21.70 and 24.07, which was related to PCL diffraction. The crystallinities of PCL and TPS/PCL composites were calculated from the ratio of the main crystalline peak areas to the overall diffraction area according to Eq. (2). Based on Eq. (2), the crystallinity of the samples ranged from 58.50% to 28.24% with increasing TPS content (Fig. 6b). The variation in the crystallinity of PCL system indicates that the incorporation of TPS made the blends progressively less crystalline than PCL. This slight decrease in the observed crystallinity was probably caused by the insertion of TPS between PCL chains. Thus, the regularity of the PCL chains is disturbed. This disturbance results in the difficulty of the PCL segments to reorganize themselves to form crystalline regions, or crystallites, in the presence of TPS. Thus, the addition of TPS can decrease the crystallization ability of PCL during the crystallization processes.

3.5. Dynamic isothermal crystallization analysis

Fig. 7a shows the isothermal crystallization thermograms of the PCL and TPS/PCL composites. The thermograms were obtained by cooling a molten polymer to the designated crystallization temperature (T_c). T_c affects PCL crystallization, and the influence of T_c on crystallization is similar for both PCL and TPS/PCL blends. The crystallization exothermic peak roughly shifts to a higher value with increasing T_c, as shown in Fig. 7a. So this shows that the crystallization of pure PCL is strongly influenced by the addition of TPS. This result is in agreement with the previous conclusion (XRD testing) on that. However, the addition of TPS shortens the time to reach the half-degree of crystallization, which indicates a faster crystallization rate shown in Table 1 (except for SP0). To some extent, this is due to the synergetic effect of the starch for nucleating the crystallization. In the blends system, TPS can constrain the movement of the PCL chain to decrease its crystallization ability, meanwhile also may function as a nucleating agent and contribute to an improvement in the crystallinity of the PCL matrix.

Usually, the isothermal crystallization kinetics of polymers and polymer composites can be better visualized by evaluating the relative degree of crystallinity as a function of time at a constant temperature. The relative crystallinity (X_t) versus a different crystallization time (t) is defined as the following equation:

$$X_t = \frac{Q_t}{Q_\infty} = \frac{\int_0^t (dH_c/dt)dt}{\int_0^{t_\infty} (dH_c/dt)dt} \tag{3}$$

where Q_t and Q_∞ represent the heat generated at time t and infinity, respectively, and dH_c/dt is the rate of heat evolution. X_t is obtained from the exothermic peak area of the isothermal crystallization analysis in DSC and is plotted in Fig. 7b. As shown in Fig. 7b, all curves have the same "S" shape. The characteristic sigmoidal isotherms roughly shift to the right along the time axis with increasing T_c. This curve indicates that the crystallization rate decreases.

The classical Avrami theory is usually employed to analyze the crystallization kinetics of polymers and polymer composites. Considering that relative crystallinity (X_t) increases over the crystallization time (t), this theory can be used to study the isothermal crystallization process of pure PCL and TPS/PCL blends (Avrami, 1939, 1940, 1941; Huang, Gu, & Ozaki, 2006), as given in Eq. (4):

$$1 - X_t = \exp(-Kt^n) \tag{4}$$

where n and K values are the Avrami exponent and the crystallization rate constant, respectively. n is a mechanism constant dependent on the form of nucleation and crystal growth, and K is a growth rate constant dependent on the growth rate parameters and nucleation. X_t denotes the relative crystallinity of the polymers at different times or temperatures, and t is the period of crystallization.

The crystallization process of polymers is usually divided into two stages, namely, the primary crystallization stage (linear portion) and the secondary crystallization stage (nonlinear portion). The linear portion is attributed to the outward clear growth of lamellar stacks. The nonlinear portion caused by the occurrence of secondary crystallization is due to the spherulite impingement and the perfection of the internal spherulite crystallization in the later stage of the crystallization process (Run, Song, Wang, Bai, & Jia, 2009). However, the Avrami equation is generally considered to be applicable only for the primary crystallization stage.

In order to deal conveniently with the operation, Eq. (4) is usually rewritten in a double logarithmic form as follows:

$$\ln[-\ln(1 - X_t)] = \ln\ K + n\ \ln\ t \tag{5}$$

The plot of $\ln[-\ln(1-X_t)]$ versus $\ln t$ for each cooling rate (according to Eq. (5)) is shown in Fig. 6c. With regard to the isothermal crystallization process, a linear portion is about 30–70% of the relative crystallinity (Liao, Yang, Yu, & Zhou, 2007). Therefore, our current study only focuses on the linear relationship of $\ln[-\ln(1-X_t)]$ versus $\ln t$ plots for the isothermal crystallization behavior of PCL and TPS/PCL composites. From the slope and intercept of the lines, the Avrami exponent n and the crystallization rate K are determined and shown in Table 1.

The crystallization half-time ($t_{1/2}$) is another important crystallization kinetics parameter. $t_{1/2}$ is defined as the time at which the extent of crystallization is 50%. $t_{1/2}$ is used to characterize the crystallization rate and can be derived from the following equation:

$$t_{1/2} = \left(\frac{\ln\ 2}{K}\right)^{1/n} \tag{6}$$

Furthermore, the growth rate of crystallization ($\tau_{1/2}$) is obtained from the reciprocal of $t_{1/2}$, as follows:

$$\tau_{1/2} = \frac{1}{t_{1/2}} \tag{7}$$

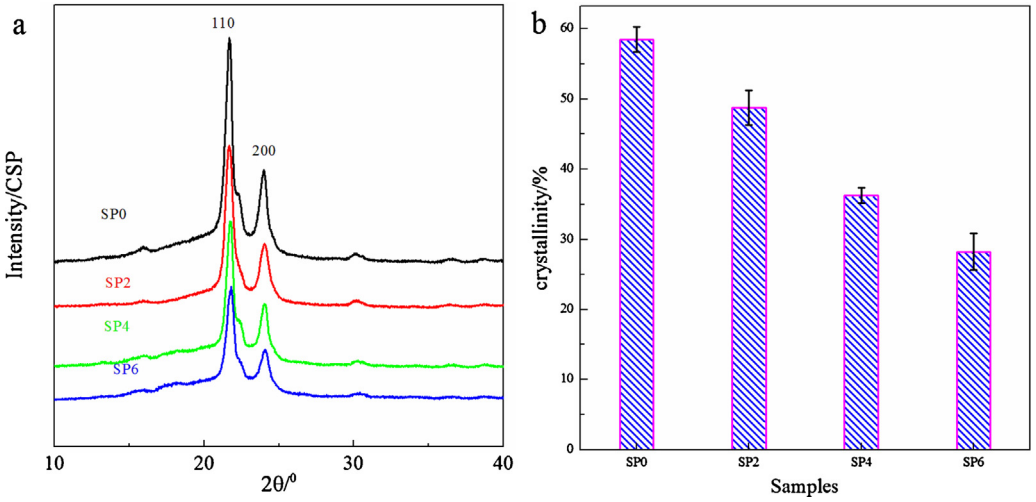

Fig. 6. XRD curves (a) and the crystallinity degree (b) of SP0, SP2, SP4, and SP6.

The dependence of $t_{1/2}$ and $\tau_{1/2}$ on T_c for four samples from the above equations is listed in Table 1. A longer $t_{1/2}$ indicates a lower $\tau_{1/2}$.

In the Avrami equations, n indicates the qualitative information on the growth processes and the nature of nucleation (Ge, Ding, Shi, & Fu, 2009; Zou et al., 2009). n with a value close to 3 is related to the three-dimensional crystal growth (spherical structure) caused by instantaneous a thermal nucleation process. n between 2 and 3 denotes non-three-dimensional truncated spherical structures that result from instantaneous nucleation controlled by diffusion. Non-integral values of n indicate a combination of thermal and athermal mixed nucleation and mechanisms (Kalkar, Deshpande, & Kulkarni, 2009; Liu et al., 2010).

As shown in Table 1, the obtained values for n are very close to one another and range from 1.8 to 2.6. This result indicates the gradual crystal growth of a two-dimensional morphology to a spherical three-dimensional morphology with a combination of thermal and athermal nucleation in the TPS/PCL blends. The n values reported in the literature were dispersed and ranged from 1.8 to 2.7. The inconformity in values is due to several factors such as the crystal growth form, the nucleation mechanism, and the difference in techniques. Thus, the obtained n values in this study are acceptable.

The K values, which are related to nucleation rate and growth processes, were extremely sensitive to T_c (Table 1). K decreases in all TPS/PCL composites with increasing T_c, which indicates a decreasing crystallization rate. The addition of TPS significantly increases K, which indicates that TPS functions as an effective nucleating agent that accelerates the crystallization rate of PCL by reducing the melt viscosity and by providing nucleating sites.

As shown in Table 1, the $t_{1/2}$ values increase with increasing T_c. This result indicates that the crystallization rate decreases in most samples. The $t_{1/2}$ values of the composites are lower than those of pure PCL, which indicates that TPS accelerates PCL crystallization in the system. This result is in accordance with those of previous studies. The results in Table 1 are also consistent with those inferred from Fig. 6b.

The activation energy for isothermal crystallization was evaluated using the following form of the Arrhenius equation:

$$K^{1/n} = K_0 \exp\left(-\frac{\Delta E_a}{RT_c}\right) \tag{8}$$

where T_c denotes crystallization temperature. K and K_0 values are crystallization rate constant and pre-exponential factor, respectively. R is the universal gas constant, and ΔE_a is the total apparent activation energy. $\Delta E_a = \Delta F + \Delta\varphi$, where, $\Delta\varphi$ is the nucleation activation energy or the activation energy for forming critical sized nuclei at crystallization temperature T_c, and ΔF is the transformation activation energy or the activation energy of a unit crystallite crossing through the liquid–solid interface of a polymer. At a high crystallization temperature from the melt, the nucleation activation energy $\Delta\varphi/(RT_c)$ is dominant at a very low supercool degree and $\Delta F/(RT_c)$ in the multinomial expression becomes negligible. Thus, $\Delta\varphi$ approximately expresses the total activation energy ΔE_a.

Rearranging Eq. (8) as follows is most convenient:

$$\frac{1}{n}\ln\ K = \ln(K_0) - \frac{\Delta E_a}{RT_c} \tag{9}$$

In our study, the crystallization activation energy (ΔE_a) is determined by the slopes of the plots of $(1/n)$ ln K versus $1/T_c$ by the Arrhenius equation (8). The ΔE_a values for neat PCL and TPS/PCL composites for primary crystallization are listed in Table 1.

Table 1 shows that the ΔE_a values are negative because the system releases energy when the polymer melt transforms into a crystalline state. Compared with neat PCL, the TPS/PCL composites have higher ΔE_a values. This result indicates that ΔE_a is dependent on the introduction of TPS into the PCL composites. In the PCL matrix, the collision and intercross of TPS hinder the movement and rearrangement of the PCL chain, which could lead to a drop in the crystallization ability of PCL during the crystallization processes. This result is also in accordance with those of XRD analysis.

4. Conclusions

In this study, the effect of TPS on the structure, thermal properties, morphology and crystallization behavior of TPS/PCL composites were investigated by Fourier transform infrared (FTIR) spectroscopy, thermogravimetric analysis (TGA), scanning electron microscopy (SEM), X-ray diffraction (XRD) and differential scanning calorimetry (DSC). FTIR confirmed the existence of the interaction between PCL and TPS, whereas TGA showed that the thermal stability was decreased by the addition of TPS. In addition, morphological analysis revealed a good dispersion of the polymers, but weak interfacial adhesion with increasing TPS. The overall crystallization rate, crystallization ability and crystallization activation energy (ΔE_a) of PCL composites were remarkably affected because of TPS incorporation. The XRD analysis indicated that the crystallinity degree of the composites decreased from 58.50% to 28.24% with the increase TPS content. Compared with neat PCL, all TPS/PCL composites had lower crystallinity degree values, which indicate

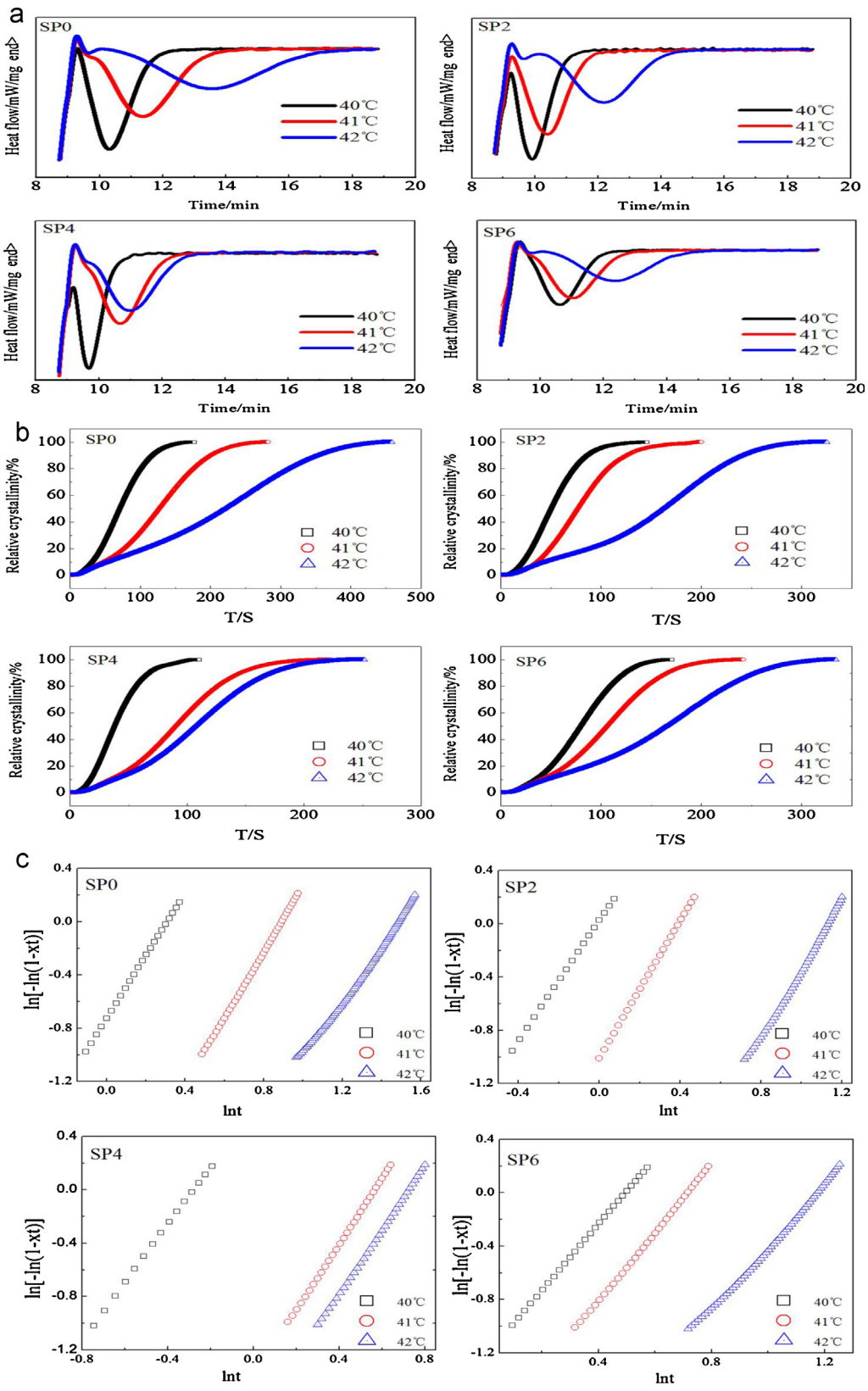

Fig. 7. (a) The DSC traces of samples isothermally crystallized at the specified temperature. (b) Plots of X_t versus t for the isothermal crystallization of samples at the specified temperature. (c) Plots of $\ln[-\ln(1-X_t)]$ versus $\ln t$ for the isothermal crystallization of samples at the specified temperature.

that mobility constraints exist in the PCL chains. Thus, the crystallization ability of PCL composites decreases because of the presence of TPS. The Avrami exponent n values of the TPS/PCL composites obtained in the study are in the range of 1.8 to 2.6. It is implied that a non three-dimensional truncated spherical structures resulting from instantaneous nucleation controlled by diffusion process. The addition of TPS significantly increases K, which indicates that TPS functions as an effective nucleating agent that accelerates the

crystallization rate of PCL in composites. The crystallization half-time values ($t_{1/2}$) values of the composites are lower than those of pure PCL. Thus, TPS accelerates PCL crystallization in the system. It is the same to previous studies. At the same time, ΔE_a was calculated from the Arrhenius formula, and the TPS/PCL composites have a higher value than those of neat PCL. In the PCL matrix, the collision and intercross of TPS hinder the movement and rearrangement of the PCL chain, which could lead to a drop in the crystallization ability of PCL during the crystallization processes. This result is also in accordance with those of XRD analysis.

Acknowledgments

The authors gratefully acknowledge the financial assistance supported by the National Science and Technology Support Program (No. 2012BAD54G01), the Fundamental Research Funds for the Central Universities (No. 2011PY152), the Huazhong Agricultural University Scientific & Technological Self-innovation Foundation (No. 2012SC21), the Chinese Scholarship Council during his visit to Deakin University, and the National Natural Science Foundation of China (No. 20976066).

References

Avella, M., Errico, M. E., Rimedio, R., & Sadocco, P. (2002). Preparation of biodegradable polyesters/high-amylose-starch composites by reactive blending and their characterization. *Journal of Applied Polymer Science*, *83*(7), 1432–1442.

Avrami, M. (1939). Kinetics of phase change. I. General theory. *Journal of Chemical Physics*, *7*(12), 1103–1113.

Avrami, M. (1940). Kinetics of phase change. II. Transformation-time relations for random distribution of nuclei. *Journal of Chemical Physics*, *8*(2), 212–225.

Avrami, M. (1941). Granulation, phase change, and microstructure kinetics of phase change (III). *Journal of Chemical Physics*, *9*(2), 177–184.

Cao, X., Mohamed, A., Gordon, S. H., Willett, J. L., & Sessa, D. J. (2003). DSC study of biodegradable poly(lactic acid) and poly(hydroxy ester ether) blends. *Thermochimica Acta*, *406*(1), 115–127.

De, K. C., Vander, W. C., & David, C. (1997). Biodegradation of poly(ε-caprolactone) and its blends with poly(vinylalcohol) by micro-organisms from a compost of house-hold refuse. *Polymer Degradation and Stability*, *55*(1), 107–113.

Del, N. M. A., Contea, A., Buonocore, G. G., Incoronato, A. L., Massaro, A., & Panza, O. (2009). Active packaging by extrusion processing of recyclable and biodegradable polymers. *Journal of Food Engineering*, *93*(1), 1–6.

Elsenhaber, F., & Schulz, W. (1993). Monte Carlo simulation of the hydration shell of double-helical amylase: A left-handed antiparallel double helix fits best into liquid water the basis of two crystalline phase (Ia/Iβ) system. *Journal of Applied Polymer Science*, *49*(8), 1491–1496.

Flemming, H. C. (1998). Relevance of biofilms for the biodeterioration of surfaces of polymeric materials. *Polymer Degradation and Stability*, *59*(1), 309–315.

Ge, C. H., Ding, P., Shi, L. Y., & Fu, J. F. (2009). Isothermal crystallization kinetics and melting behavior of poly(ethylene terephthalate)/barite nanocomposites. *Journal of Polymer Science Part B: Polymer Physics*, *47*(7), 665–668.

Heartwin, A. P., Pratik, B., & Milford, A. H. (2010). Effects of LDPE and glycerol contents and compounding on the microstructure and properties of starch composite films. *Carbohydrate Polymers*, *82*(4), 1082–1089.

Horowitz, H. H., & Metzger, G. (1963). A new analysis of thermogravimetric traces. *Analytical Chemistry*, *35*(10), 1464–1468.

Huang, H., Gu, L. X., & Ozaki, Y. (2006). Non-isothermal crystallization and thermal transitions of a biodegradable, partially hydrolyzed poly(vinyl alcohol). *Polymer*, *47*(11), 3935–3945.

Huang, C. Y., Roan, M. L., Kuo, M. C., & Lu, W. L. (2005). Effect of compatibiliser on the biodegradation and mechanical properties of high-content starch/low-density polyethylene blends. *Polymer Degradation and Stability*, *90*(1), 95–105.

Ishiaku, U. S., Pang, K. W., Lee, W. S., & Ishak, M. (2002). Mechanical properties and enzymic degradation of thermoplastic and granular sago starch filled poly(e-caprolactone). *European Polymer Journal*, *38*(2), 393–401.

Joseph, C. S., Prashanth, H. K. V., Rastogi, N. K., Indiramma, A. R., Reddy, S. Y., & Raghavarao, K. S. M. S. (2011). *Food and Bioprocess Technology*, *4*(7), 1179–1185.

Kalkar, A. K., Deshpande, V. D., & Kulkarni, M. J. (2009). Isothermal crystallization kinetics of poly(phenylene sulfide)/TLCP composites. *Polymer Engineering and Science*, *49*(2), 397–417.

Ke, T. Y., & Sun, X. Z. (2000). Physical properties of poly(lactic acid) and starch composites with various blending ratios. *Cereal Chemistry*, *77*(6), 761–768.

Kumar, M., Mohanty, S., Nayak, S. K., & Parvaiz, M. R. (2010). Effect of glycidyl methacrylate (GMA) on the thermal, mechanical and morphological property of biodegradable PLA/PBAT blend and its nanocomposites. *Bioresource Technology*, *101*(21), 8406–8415.

Leloup, V. M., Colonna, P., & Ring, S. (1991). α-Amylase adsorption on starch crystallites. *Biotechnology and Bioengineering*, *38*(2), 127–134.

Liao, R. G., Yang, B., Yu, W., & Zhou, C. X. (2007). Isothermal cold crystallization kinetics of polylactide/nucleating agents. *Journal of Applied Polymer Science*, *104*(1), 310–317.

Liu, Z., Dong, Y., Men, H., Jiang, M., Tong, L., & Zhou, J. (2012). Post-crosslinking modification of thermoplastic starch/PVA blend films by using sodium hexametaphosphate. *Carbohydrate Polymers*, *89*(2), 473–477.

Liu, H. X., Huang, Y. Y., Yuan, L., He, P. S., Cai, Z. H., Xu, Y. M., et al. (2010). Isothermal crystallization kinetics of modified bamboo cellulose/PCL composites. *Carbohydrate Polymers*, *79*(3), 513–519.

Luo, X., Li, J., & Lin, X. (2012). Effect of gelatinization and additives on morphology and thermal behavior of corn starch/PVA blend films. *Carbohydrate Polymers*, *90*(4), 1595–1600.

Mahieu, A., Terrié, C., Agoulon, A., Leblanc, N., & Youssef, B. (2013). Thermoplastic starch and poly(ε-caprolactone) blends: Morphology and mechanical properties as a function of relative humidity. *Journal of Polymer Research*, *229*(20), 1–13.

Mano, J. F., Koniarova, D., & Reis, R. L. (2003). Thermal properties of thermoplastic starch/synthetic polymer blends with potential biomedical applicability. *Journal of Materials Science: Materials in Medicine*, *14*(3), 127–135.

Nakamura, E. M., Cordi, L., Almeida, G. S. G., Duran, N., & Mei, L. H. I. (2005). Study and development of LDPE/starch partially biodegradable compounds. *Journal of Materials Processing Technology*, *162–163*, 236–241.

Nakayama, A., Kawasaki, N., Maeda, Y., Arvanitoyannis, I., Ariba, S., & Yamamoto, N. (1997). Nonisothermal crystallization kinetics of modified bamboo fiber/PCL composites? *Journal of Applied Polymer Science*, *116*(4), 2119–2125.

Pedroso, A. G., & Rosa, D. S. (2005). Mechanical, thermal and morphological characterization of recycled LDPE/corn starch blends. *Carbohydrate Polymers*, *59*(1), 1–9.

Peter, L., Krishnan, J., & Debes, B. (2009). Water-free blending of thermoplastic starch and polyethylene for rotomoulding. *Starch/Stärke*, *61*, 43–45.

Rhim, J. W., Park, H. M., & Ha, C. S. (2013). Bio-nanocomposites for food packaging applications. *Progress in Polymer Science*, *38*(10), 1629–1652.

Rosa, D. S., Rodrigues, T. C., Guedes, C. G. F., & Calil, M. R. (2003). Effect of thermal aging on the biodegradation of PCL, PHB-V, and their blends with starch in soil compost. *Journal of Applied Polymer Science*, *89*(13), 3539–3546.

Run, M. T., Song, H. Z., Wang, S. J., Bai, L. B., & Jia, Y. H. (2009). Crystal morphology, melting behaviors and isothermal crystallization kinetics of SCF/PTT composites. *Polymer Composites*, *30*(1), 87–94.

Suprakas, S. R., Kazunobu, Y., Masami, O., Akinobu, O., & Kazue, U. (2003). New polylactide/layered silicate nanocomposite: Nanoscale control over multiple properties. *Macromolecular Rapid Communications*, *23*(16), 943–947.

Tamai, N., Aono, H., Tatsumi, D., & Matsumoto, T. (2003). Differences in rheological properties of solutions of plant and bacterial cellulose in LiCl/N,N-dimethylacetamide. *Journal of the Society of Rheology*, *31*(3), 119–130.

Wang, S., & Yu, J. (2005). Compatible thermoplastic starch/polyethylene blends by one-step reactive extrusion. *Polymer International*, *54*(2), 279–285.

Xiong, H. G., Tang, S. W., Tang, H. L., & Zou, P. (2008). The structure and properties of a starch-based biodegradable film. *Carbohydrate Polymers*, *71*(2), 263–268.

Yoon, S. D., Park, M. H., & Byun, H. S. (2012). Mechanical and water barrier properties of starch/PVA composite films by adding nano-sized poly(methyl methacrylate-co-acrylamide) particles? *Carbohydrate Polymers*, *87*(1), 676–686.

Zou, P., Tang, S. W., Fu, Z. Z., & Xiong, H. G. (2009). Isothermal and non-isothermal crystallization kinetics of modified rape straw flour/high-density polyethylene composites. *International Journal of Thermal Sciences*, *48*(4), 837–846.